Original Article

MOLECULAR METABOLISM

NNT reverse mode of operation mediates glucose control of mitochondrial NADPH and glutathione redox state in mouse pancreatic β-cells

Laila R.B. Santos [1,5,6], Carole Muller [1,5], Arnaldo H. de Souza [1,7], Hilton K. Takahashi [1,8], Peter Spégel [2,3], Ian R. Sweet [4], Heeyoung Chae [1], Hindrik Mulder [2], Jean-Christophe Jonas [1,*]

ABSTRACT

Objective: The glucose stimulation of insulin secretion (GSIS) by pancreatic β-cells critically depends on increased production of metabolic coupling factors, including NADPH. Nicotinamide nucleotide transhydrogenase (NNT) typically produces NADPH at the expense of NADH and ΔpH in energized mitochondria. Its spontaneous inactivation in C57BL/6J mice was previously shown to alter ATP production, Ca^{2+} influx, and GSIS, thereby leading to glucose intolerance. Here, we tested the role of NNT in the glucose regulation of mitochondrial NADPH and glutathione redox state and reinvestigated its role in GSIS coupling events in mouse pancreatic islets.

Methods: Islets were isolated from female C57BL/6J mice (J-islets), which lack functional NNT, and genetically close C57BL/6N mice (N-islets). Wild-type mouse NNT was expressed in J-islets by adenoviral infection. Mitochondrial and cytosolic glutathione oxidation was measured with glutaredoxin 1-fused roGFP2 probes targeted or not to the mitochondrial matrix. NADPH and NADH redox state was measured biochemically. Insulin secretion and upstream coupling events were measured under dynamic or static conditions by standard procedures.

Results: NNT is largely responsible for the acute glucose-induced rise in islet NADPH/$NADP^+$ ratio and decrease in mitochondrial glutathione oxidation, with a small impact on cytosolic glutathione. However, contrary to current views on NNT in β-cells, these effects resulted from a glucose-dependent reduction in NADPH consumption by NNT reverse mode of operation, rather than from a stimulation of its forward mode of operation. Accordingly, the lack of NNT in J-islets decreased their sensitivity to exogenous H_2O_2 at non-stimulating glucose. Surprisingly, the lack of NNT did not alter the glucose-stimulation of Ca^{2+} influx and upstream mitochondrial events, but it markedly reduced both phases of GSIS by altering Ca^{2+}-induced exocytosis and its metabolic amplification.

Conclusion: These results drastically modify current views on NNT operation and mitochondrial function in pancreatic β-cells.

© 2017 The Authors. Published by Elsevier GmbH. This is an open access article under the CC BY-NC-ND license (http://creativecommons.org/licenses/by-nc-nd/4.0/).

Keywords C57BL/6J mice; C57BL/6N mice; Glucose metabolism; GRX1-roGFP2; Insulin secretion; Mitochondrial shuttles; Pancreatic islet; Redox-sensitive GFP; Stimulus-secretion coupling

1. INTRODUCTION

The glucose stimulation of insulin secretion (GSIS) by pancreatic β-cells depends on the increased flux of glucose metabolism through glycolysis and mitochondrial Krebs cycle, leading to a rise in the NADH/NAD^+ ratio, mitochondrial membrane hyperpolarization, matrix alkalization, and ATP synthesis. The ensuing rise in the ATP/ADP ratio closes K_{ATP} channels, thereby depolarizing the plasma membrane, opening voltage-dependent Ca^{2+} channels and triggering Ca^{2+} influx, rise in intracellular Ca^{2+} concentration ($[Ca^{2+}]_i$) and insulin granule exocytosis. In addition, glucose-derived coupling factors play a role in the metabolic amplification of Ca^{2+}-induced secretion [1–4]. Among

[1]Université catholique de Louvain, Institute of Experimental and Clinical Research, Pole of Endocrinology, Diabetes and Nutrition, Brussels, B-1200, Belgium [2]Lund University, Department of Clinical Sciences in Malmö, Unit of Molecular Metabolism, Malmö, 205 02, Sweden [3]Lund University, Department of Chemistry, Centre for Analysis and Synthesis, Lund, 221 00, Sweden [4]University of Washington Diabetes Institute, Department of Medicine, University of Washington, Seattle, WA, 98195, USA

[5] Laila R.B. Santos and Carole Muller contributed equally to this work.
[6] Present address: Institute for Vascular Signalling, Centre for Molecular Medicine, Goethe University, Frankfurt am Main, Germany.
[7] Present address: MitoCare Center, Department of Pathology, Anatomy and Cell Biology, Thomas Jefferson University, Philadelphia, PA, USA.
[8] Present address: Department of Physiology and Biophysics, Institute of Biomedical Sciences, University of São Paulo, Brazil.

*Corresponding author. Université catholique de Louvain, UCL/SSS/IREC/EDIN, Avenue Hippocrate 55, B1.55.06, B-1200, Brussels, Belgium. E-mail: jean-christophe.jonas@uclouvain.be (J.-C. Jonas).

Abbreviations: AT2, aldrithiol; CMV, cytomegalovirus; Dz, diazoxide; DTT, dithiotreitol; FCCP, carbonyl cyanide-p-trifluoromethoxyphenylhydrazone; GSIS, glucose stimulation of insulin secretion; GRX1, glutaredoxin 1; $[Ca^{2+}]_i$, intracellular Ca^{2+} concentration; IDH, isocitrate dehydrogenase; KRB, Krebs solution; ME, malic enzyme; WT, wild-type; NNT, nicotinamide nucleotide transhydrogenase; OCR, oxygen consumption rate

Received February 28, 2017 • Revision received April 10, 2017 • Accepted April 18, 2017 • Available online 21 April 2017

http://dx.doi.org/10.1016/j.molmet.2017.04.004

 © 2017 The Authors. Published by Elsevier GmbH. This is an open access article under the CC BY-NC-ND license (http://creativecommons.org/licenses/by-nc-nd/4.0/).

them, cytosolic NADPH together with glutaredoxin 1 (GRX1) acts as a regulatory or permissive factor for Ca^{2+}-induced exocytosis [5—7], an effect which may result from protein deSUMOylation by redox-sensitive SENP-1 [8,9].

Using the glutathione redox probe GRX1-roGFP2, we showed that the rise in NAD(P)H autofluorescence, which mainly occurs in mitochondria [10], correlates with a decrease in mitochondrial glutathione oxidation in rat and human β-cells, suggesting that mitochondrial NAD(P)H and glutathione redox state may play a role in GSIS [11]. Mitochondrial NADPH is typically produced by nicotinamide nucleotide transhydrogenase (NNT), isocitrate dehydrogenase (IDH) 2 and malic enzyme (ME) 3 [3,12]. Interestingly, the spontaneous inactivating mutation of NNT in C57BL/6J mice (J-mice) impairs their GSIS and glucose tolerance, a defect that was ascribed to mitochondrial oxidative stress and impaired glucose-induced ATP production and Ca^{2+} influx [13,14]. As NNT catalyzes the reversible transfer of a hydride from NADH to $NADP^+$ coupled to proton influx in the matrix of energized mitochondria [15,16], we hypothesized that NNT could mediate the decrease of mitochondrial glutathione oxidation by glucose stimulation, so that islets from J-mice would allow testing the role of mitochondrial NADPH and glutathione redox state in GSIS.

Here, comparing islets from C57BL/6J mice and their parental C57BL/6N mice that express functional wild-type (WT) NNT, we show that the enzyme mediates the effects of glucose on islet NADPH and mitochondrial glutathione redox state, but that, contrary to current views on NNT in β-cells, it does so by reducing its reverse mode of operation, which consumes NADPH, from non-stimulating to stimulating glucose concentrations. We also show that the lower GSIS in J-islets results from alterations of Ca^{2+}-induced exocytosis and its metabolic amplification despite the preservation of glucose-induced ATP production and rise in $[Ca^{2+}]_i$.

2. MATERIALS AND METHODS

2.1. Animals

Animal experiments were approved by the local Institutional Committee on Animal Experimentation (Project 2013/UCL/MD/016). Female C57BL/6N mice expressing WT NNT ($NNT^{wt/wt}$) and C57BL/6J mice with truncated NNT ($NNT^{tr/tr}$) originated from the Jackson Laboratory (Strain 005304 (NJ) and 000664 (J)) or from Janvier Labs, Le Genest Saint Isle, France (C57BL/6NRj and C57BL/6JRj). Mice heterozygous for NNT truncation ($NNT^{wt/tr}$) were obtained by crossing C57BL/6NRj with C57BL/6JRj. Mice were matched for age in each experiment, and their NNT genotype was checked by tail-DNA PCR (standard PCR genotyping protocol for strain 000664, Jackson Laboratory website). $NNT^{wt/wt}$, $NNT^{tr/tr}$ and $NNT^{wt/tr}$ mice are referred to as N-, J- and N/J-mice, and their islets accordingly.

2.2. Reagents

Dithiotreitol (DTT), aldrithiol (AT2), diazoxide (Dz) and carbonyl cyanide-p-trifluoromethoxyphenylhydrazone (FCCP) were from Sigma. Other reagents were from Merck. A rabbit polyclonal antibody recognizing a synthetic antigen from mouse NNT was kindly provided by Dr. Ting—Ting Huang, Stanford Neuroscience Institute, CA [17]. Rabbit anti-actin antibody (A 2066) was from Sigma.

2.3. Adenoviruses

The generation and amplification of adenoviruses coding GRX1—roGFP2, mt-GRX1—roGFP2, or mt-SypHer under the control of the cytomegalovirus (CMV) promoter and of an adenovirus coding the red fluorescent protein DsRed under the control of the rat insulin promoter (Ad-RIP-DsRed) were described previously [11,18,19]. Adenoviruses coding WT mouse NNT together with mCherry (Ad-NNT) or mCherry alone (Ad-mCh) under the control of the CMV promoter were from Vector Biolabs (Philadelphia, PA).

2.4. Islet isolation

Islets were isolated by collagenase digestion of the pancreas followed by density gradient centrifugation using Histopaque 1077. They were cultured for 2—5 days at 37 °C and 5% CO_2 in standard RPMI 1640 (Invitrogen) supplemented with 2 mmol/l glutamine, 100 U/ml penicillin, 100 μg/ml streptomycin, and 5 g/l BSA.

2.5. Expression of WT mouse NNT in J-islets

After overnight culture in RPMI medium, J-islets were infected with Ad-NNT or Ad-mCh as control, at multiplicity of infection ~100. After 2—4 days of culture, the fluorescence of islet cells was checked by confocal microscopy (λexc/em 561/625—685 nm).

WT *Nnt* and *Tbp* mRNA levels were measured by real-time RT-PCR using iQ supermix and a CFX96 thermocycler (Biorad), and the *Nnt/Tbp* mRNA ratio was computed as $2^{-(Ct_{Nnt}-Ct_{Tbp})}$. Primers for WT *Nnt* were designed in part of the coding sequence of mouse *Nnt* that is truncated in J-mice (sense 5′-gCTCCCACACCAAAAAATATTCCg-3′ and antisense 5′-TACAATCCAAACCCgTAgCACCg-3′).

NNT and actin protein levels were measured by western blot. Briefly, islets and heart extracts were separated on a 7% polyacrylamide gel and transferred on a PVDF membrane. The membrane was blocked with 5% non-fat milk in Tris-buffered saline with 0.1% Tween 20, cut in two and incubated with NNT or actin antibody, rinsed, and further incubated with an anti-rabbit peroxidase-conjugated antibody. The chemiluminescent signal was quantified and the NNT to actin ratio computed (see Suppl. Experimental Procedures).

2.6. Solutions

Experiments were carried out in a Krebs solution (KRB) containing 120 mmol/l NaCl, 4.8 mmol/l KCl, 2.5 mmol/l $CaCl_2$, 1.2 mmol/l $MgCl_2$, 24 mmol/l $NaHCO_3$, 1 g/l BSA (fraction V; Roche), and glucose (Gn, n mmol/l glucose). When KCl was raised to 30 mmol/l, NaCl was reduced to 94.8 mmol/l. The solutions were continuously gassed with 6% CO_2 in pure O_2 to maintain pH 7.4.

2.7. Insulin secretion

J- and N-islets were preincubated 40 min in G0.5 and incubated 1 h, in batches of 5, under various conditions. The medium was collected for RIA measurement of insulin, islets were disrupted by sonication in 10 mmol/l Tris, 0.2 mol/l NaCl, 10 mmol/l EDTA, and their insulin and DNA contents were measured. For dynamic measurements, batches of 35 J- and N-islets were perifused in parallel with KRB at a flow rate of 1 ml/min. Insulin was measured on the effluent collected every 2 min. The islet DNA and insulin contents were measured at the end of perifusion as described [20].

2.8. Live-cell imaging (NAD(P)H autofluorescence, intracellular Ca^{2+} concentration, mitochondrial and cytosolic glutathione oxidation, mitochondrial pH)

After culture, islets from N- and J-mice were simultaneously perifused side by side with KRB at a flow rate of ~1 ml/min and at 37 °C

 © 2017 The Authors. Published by Elsevier GmbH. This is an open access article under the CC BY-NC-ND license (http://creativecommons.org/licenses/by-nc-nd/4.0/).

on the stage of an inverted microscope. NAD(P)H autofluorescence (λex/em 360/470 nm) was measured every 5 s and normalized to the fluorescence level measured in N-islets at G0.5. To measure intracellular Ca^{2+} concentration ($[Ca^{2+}]_i$), the islets were loaded for 2 h with 2 μmol/l Fura-2 LR acetoxymethyl ester (Teflabs), and the fluorescence ratio (λex/em 340/510 and 380/510 nm) was measured every 5 s [21]. To measure glutathione oxidation, the fluorescence ratio of (mt-)GRX1—roGFP2 (λex/em 400/535 and 480/535 nm) was measured every 30 s in islets infected 48—72 h earlier with Ad-(mt-)GRX1—roGFP2 (multiplicity of infection ~100) as described [11,22]. The results were normalized to the fluorescence ratio of the maximally reduced probe measured in the presence of 10 mmol/l DTT (set to 0%), and that of the maximally oxidized probe measured in the presence of 100 μmol/l AT2 (set to 100%). For relative changes in mitochondrial pH, the fluorescence ratio of mt-SypHer (λex 480/405 nm; λem 535 nm) was recorded every 30 s in islets previously infected with Ad-mt-SypHer as described [18]. Islets were imaged through a ×20 objective with an Evolve 512 camera (Photometrics, Tucson, AZ).

2.9. Pyridine nucleotides redox state

Batches of 20 islets were preincubated 40 min in G0.5 before incubation under various conditions for 15 min. The reaction was stopped with NaOH 0.2 N and 1% DTAB and islets were briefly sonicated. NAD^+, NADH, $NADP^+$, and NADPH were assayed with the NAD/NADH-Glo™ and NADP/NADPH-Glo™ Assays (Promega) (see Suppl. Experimental Procedures).

2.10. Adenine nucleotides

Batches of 10 islets were preincubated 30 min in G0.5 then incubated 30 min under various conditions. The reaction was stopped with trichloroacetic acid, and ATP was assayed using the ATP bioluminescence assay kit CLSII (Roche Life Science) as described [21]. The sum ATP + ADP was measured on the same sample, and the ratio ATP/(ATP + ADP) was computed.

2.11. Glucose oxidation

Batches of 20 islets were incubated for 2 h at 37 °C in 100 μL KRB containing G0.5 or G30 and 1 μCi of uniformly labelled D-[U-^{14}C]-glucose. The reaction was stopped with 100 μL HCl 0.1 N, followed by 100 μL Na_2HPO_4 buffer, pH 6.0. $^{14}CO_2$ was absorbed overnight by Hyamin (Perkin Elmer) and counted by liquid scintillation. The specific activity of D-[U-^{14}C]-glucose was determined for both G0.5 and G30 conditions, and the quantity of glucose oxidized in each islet sample (pmol per islets per h) was computed.

2.12. Measurement of oxygen consumption rate (OCR)

Oxygen consumption by isolated islets was measured in a flow culture system as described [23,24].

2.13. Metabolomics

Metabolite profiling in islets was performed by gas chromatography mass spectrometry (GC/MS) as described [7]. Islets were analyzed in 3 separate batches and associated variation between batches removed by ComBat (sva package, R). Data were analyzed by orthogonal projections to latent structures discriminant analysis (OPLS-DA) in Simca P+13 (MKS Data Analytics Solutions, Umeå, Sweden). Differences between groups were further assessed by 1-way ANOVA with Tukey's multiple comparison test *post hoc*.

2.14. Statistics

Results are shown as means ± SEM for ≥6 islets from ≥3 different preparations. Outliers were excluded if they passed Grubber's test. The statistical significance of differences between conditions and islet types was assessed by 2-way ANOVA (for repeated measurements when the comparison was made between selected time points in the same trace) followed by a test of Bonferroni, unless otherwise specified. We used GraphPad Prism version 6 for Windows.

3. RESULTS

3.1. NNT reverse mode of operation largely contributes to the glucose regulation of NADPH/NADP(H) ratio in mouse pancreatic islets

We previously showed that, during stepwise glucose stimulation of rat and human β-cells, NAD(P)H autofluorescence (reflecting NADH + NADPH) is inversely correlated to mitochondrial glutathione oxidation [11]. To test the role of NNT-mediated NADPH production in these glucose effects, we first measured NAD(P)H autofluorescence in islets from C57BL/6 mice with (N-islets) and without functional NNT (J-islets). Figure 1AB shows that both islet types displayed a glucose-dependent increase in NAD(P)H autofluorescence. However, compared with N-islets of similar size that were perifused simultaneously, the NAD(P)H autofluorescence in J-islets was higher below G5 (Gn, n mmol/l glucose) and similar at G10 and above, so that its rise was ~52% lower from G0.5 to G10 and ~34% lower from G0.5 to G30. Moreover, the decrease in NAD(P)H autofluorescence triggered by the mitochondrial uncoupler FCCP was initially similar in both islet types but rapidly became much slower in J- *vs.* N-islets. These results indicated that NNT contributes largely to the rise in NAD(P)H between G0.5 and G30 and to the rapid decrease thereof upon mitochondrial uncoupling in N-islets. However, they also suggested that the lack of NNT in J-islets prevented a full decrease in NAD(P)H at low glucose rather than its increase at high glucose.

To distinguish the direct impact of NNT on mitochondrial NADPH from putative indirect effects on mitochondrial function preservation, we next measured the effects of glucose and FCCP on the reduced and oxidized forms of NAD and NADP in whole islets. We then computed the NADH/(NADH + NAD^+) and NADPH/(NADPH + $NADP^+$) ratios, next referred to as NADH/NAD(H) and NADPH/NADP(H) ratios. Figure 1C shows that glucose increased and FCCP decreased the NADH/NAD(H) ratio to similar extents in N- and J-islets, suggesting that glucose metabolism and mitochondrial function were globally preserved in the absence of NNT. These changes occurred without significant changes in total NAD(H) (Figure S1A—C).

In contrast, glucose and FCCP differently affected the NADPH/NADP(H) ratio in J- and N-islets. In N-islets, the ratio increased by 50% upon stimulation from G0.5 to G30, and this effect was partially reversed by FCCP (Figure 1D). In contrast, the NADPH/NADP(H) ratio in J-islets was elevated in G0.5 and unaffected by glucose or FCCP (Figure 1D). Again, the differences in NADPH/NADP(H) ratio were not due to changes in total NADP(H) (Figure S1D—F).

To confirm that the results in J-islets resulted from their lack of functional NNT and not from other genetic differences with N-islets [13,25], we infected J-islets with an adenovirus coding WT mouse NNT and mCherry (Ad-NNT), or mCherry alone as control (Ad-mCh). When the periphery of islets was infected by Ad-NNT (Figure S2), their NADPH/NADP(H) ratio tended to decrease at low glucose (about

 © 2017 The Authors. Published by Elsevier GmbH. This is an open access article under the CC BY-NC-ND license (http://creativecommons.org/licenses/by-nc-nd/4.0/).

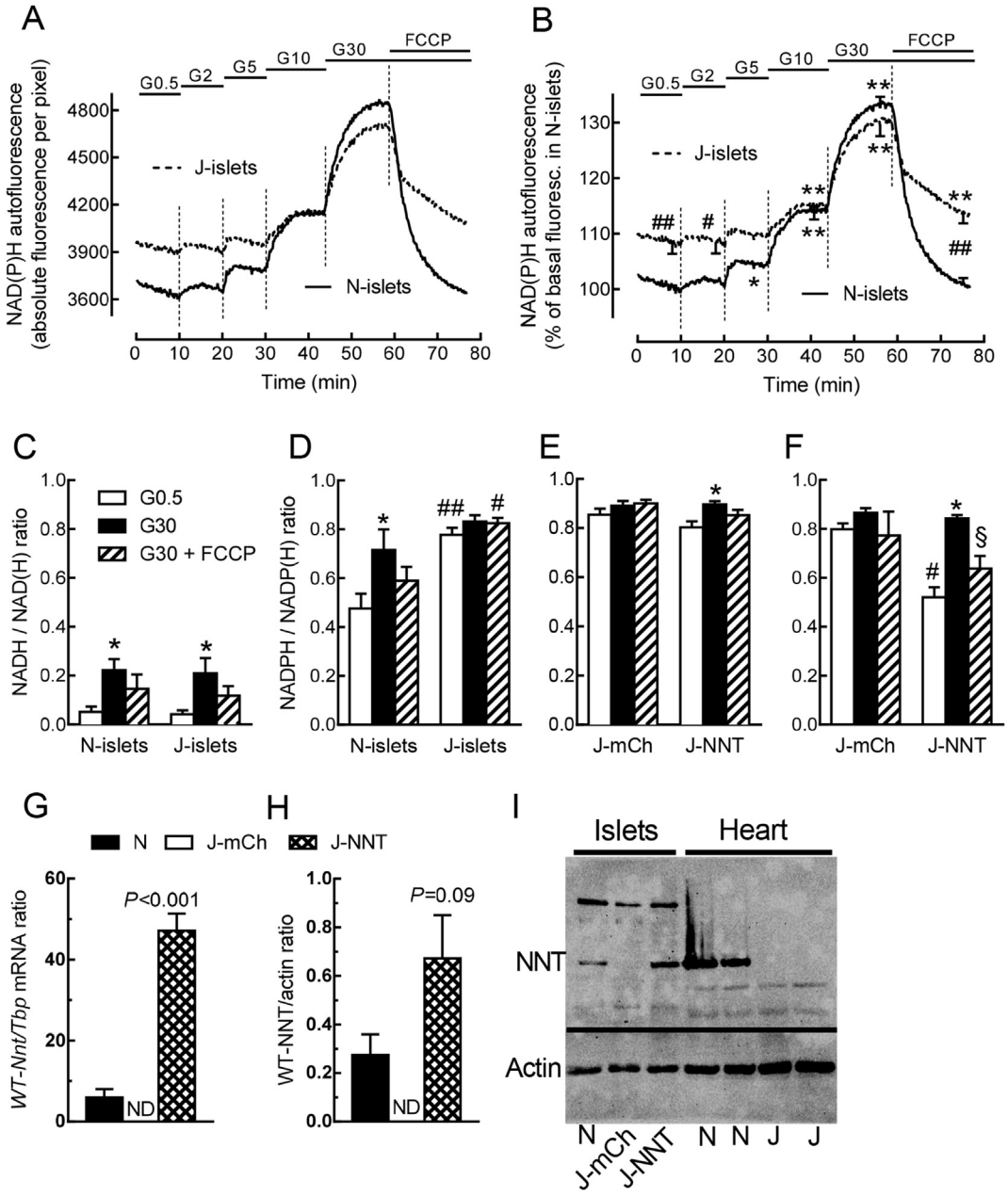

Figure 1: Effects of glucose and FCCP on pyridine nucleotides in islets from C57BL/6N and C57BL/6J mice, and impact of WT NNT expression in J-islets. N- and J-islets were perifused simultaneously in the same chamber (A, B) or incubated 15 min (C—F) in the presence of various glucose concentrations (Gn = n mmol/l glucose) or in G30 plus 10 μmol/l FCCP. Data are means (A) or means ± SEM (B—H) for n islet preparations. A, raw NAD(P)H autofluorescence levels per pixel (n = 3). B, NAD(P)H autofluorescence normalized in each experiments to the level of fluorescence in N-islets perifused with G0.5. *$P < 0.001$, **$P < 0.0001$ *vs.* G0.5, #$P < 0.05$ and ##$P < 0.01$ *vs.* N-islets (n = 3). C and D, NADH, NAD^+, NADPH and $NADP^+$ were measured in whole islet extracts and the ratios NADH/(NAD(H) and NADPH/(NADP(H) were computed. *$P < 0.05$ *vs.* G0.5; §$P < 0.05$ *vs.* G30; #$P < 0.05$, ##$P < 0.01$ *vs.* N-islets (n = 3). E and F, non-trypsinized (E) or trypsinized (F) J-islets were infected with Ad-NNT or Ad-mCh. NADPH and $NADP^+$ were measured in whole islet extracts and the ratio NADPH/(NADP(H) was computed. *$P < 0.05$, **$P < 0.001$ *vs.* G0.5; §$P < 0.05$ *vs.* G30; #$P < 0.05$ *vs.* J-mCh islets (n = 4). G—I, J-islets were infected with Ad-mCh or Ad-NNT under usual conditions (G) or after gentle trypsinisation (H and I) and further cultured for 4 days. N-islets and heart extracts from N- and J-mice were used as controls. G, the *Nnt* to *Tbp* mRNA ratio was measured by real-time RT-PCR using primers specific for WT *Nnt* (ND: not detected). *P* values were obtained by unpaired two-tailed t-test between N and J-NNT islets; n = 4. H, the NNT to actin protein ratio was measured by western blot (ND: WT NNT was not detected in J-mCh islets or J heart extracts). *P* values were obtained by unpaired two-tailed t-test between N and J-NNT islets; n = 4. I, representative blot (two parts of the same membrane).

30% of the decrease in N-islets) and in the presence of FCCP (about 45% of the decrease in N-islets) (Figure 1E). However, when islets were gently trypsinized to allow Ad-NNT infection throughout the islets (Figure S2), the decrease in NADPH/NADP(H) ratio at low glucose or by FCCP was fully restored in J-islets expressing WT NNT but not mCherry alone (Figure 1F). The level of NNT expression in N-islets and J-islets infected with Ad-mCh or Ad-NNT are shown in Figure 1G—I.

 © 2017 The Authors. Published by Elsevier GmbH. This is an open access article under the CC BY-NC-ND license (http://creativecommons.org/licenses/by-nc-nd/4.0/).

These results confirmed that NNT is critical for the effects of glucose and FCCP on islet NADPH. However, NNT did not increase NADPH at high glucose but decreased it at low glucose, suggesting that NNT operates in the reverse mode and consumes NADPH at low glucose, when the NADH/NAD^+ ratio and mitochondrial membrane potential are low in β-cells. To assess the importance of this unusual mode of NNT operation, we estimated the difference in NAD(P)H content between N- and J-islets exposed at different glucose concentrations (Figure S3AB). The results show that NADPH consumption by NNT decreased as a function of glucose concentration and became negligible at G30. About 41% of this effect occurred between G5 and G10.

3.2. NNT reverse mode of operation mediates the effect of glucose on mitochondrial glutathione oxidation in mouse β-cells, with little impact on cytosolic glutathione

We next used GRX1-roGFP2 and mt-GRX1-roGFP2 to measure the effect of glucose on cytosolic and mitochondrial glutathione oxidation. The total glutathione content was similar in N- and J-islets (4.8 ± 1.7 pg/μg protein in N-islets *vs.* 5.6 ± 1.1 pg/μg protein in J-islets, n = 3), assuring that changes in probe fluorescence ratio reflect changes in glutathione redox state [26]. Moreover, the probes were mainly expressed in islet β-cells despite the use of a CMV promoter (Figure S4).

Figure 2A shows that glucose reduced mt-GRX1-roGFP2 fluorescence ratio in N-islets as a function of concentration, reflecting a decrease in glutathione oxidation, as in rat and human β-cells [11]. About 35–40% of this effect occurred between G5 and G10. In J-islets, in contrast, mt-GRX1-roGFP2 fluorescence ratio was low at all glucose concentrations, displaying only a small increase upon glucose stimulation (Figure 2A). Again, expressing WT NNT in J-islets fully restored the glucose regulation of mt-GRX1-roGFP2 fluorescence ratio (Figure 2B), confirming the role of the enzyme in this effect. As NNT expression was higher in J-islets infected with Ad-NNT than in N-islets, we also tested the glucose responses in N/J-islets from heterozygous F1 mice obtained by crossing N- and J-mice. Figure 2C shows that the traces were almost identical in N-islets and NJ-islets, indicating that a single WT allele of *Nnt* suffices for mitochondrial glutathione oxidation at low glucose. Interestingly, FCCP only increased mt-GRX1-roGFP2 fluorescence ratio in N-islets at G30 while remaining completely ineffective in J-islets (Figure 2F). Altogether, these results support our hypothesis that NNT operates in the reverse mode below G10 as in the presence of FCCP at G30.

In contrast to the mitochondrial probe, cytosolic GRX1-roGFP2 fluorescence ratio was low and unaffected by glucose in both islet types, except for a small increase upon glucose deprivation in N- but not J-islets (Figure 2D). However, expression of WT NNT in J-islets did not restore the GRX1-roGFP2 response to glucose deprivation (Figure 2E). These results are compatible with recent data showing that the rise in cytosolic NADPH occurs between G0 and G5 [27], and indicate that the impact of NNT on cytosolic glutathione oxidation is negligible under control conditions.

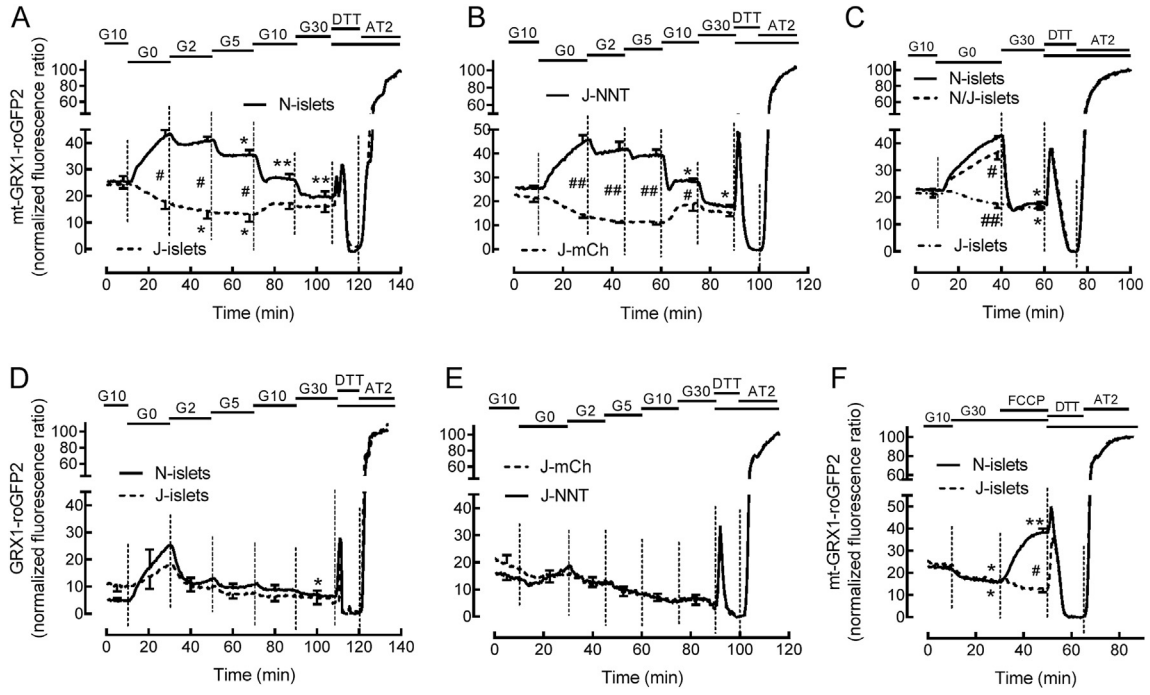

Figure 2: Effects of glucose and FCCP on mitochondrial glutathione oxidation in N- and J-islets. Islets were perifused at various glucose concentrations (Gn = n mmol/l glucose) or in G30 plus 10 μmol/l FCCP, as shown at the top of the graphs. At the end of experiments, the probe was maximally reduced with DTT (10 mmol/l) then maximally oxidized with aldrithiol (AT2, 100 μmol/l) for normalization of the traces. Data are means ± SEM for n islet preparations. A, N- and J-islets were infected with Ad-mt-GRX1-roGFP2. *$P < 0.05$, **$P < 0.0001$ *vs.* G0; #$P < 0.0001$ *vs.* N-islets (n = 4). B, J-islets were infected with Ad-mt-GRX1-roGFP2 and either Ad-NNT (J-NNT) or Ad-mCh (J-mCh) without trypsinization. *$P < 0.0001$ *vs.* G0; #$P < 0.05$, ##$P < 0.0001$ *vs.* J-mCh islets (n = 4). C, N-, N/J- and J-islets were infected with Ad-mt-GRX1-roGFP2. *$P < 0.0001$ *vs.* G0; #$P < 0.05$, ##$P < 0.0001$ *vs.* N-islets (n = 3). D, N- and J-islets were infected with Ad-GRX1-roGFP2. *$P < 0.05$ *vs.* G0 (n = 3). E, J-islets were infected with Ad-GRX1-roGFP2 and either Ad-NNT (J-NNT) or Ad-mCh (J-mCh) without trypsinization (n = 4). F, N- and J-islets were infected with Ad-mt-GRX1-roGFP2. *$P < 0.01$ *vs.* G10; **$P < 0.0001$ *vs.* G30; #$P < 0.0001$ *vs.* N-islets (n = 3).

 © 2017 The Authors. Published by Elsevier GmbH. This is an open access article under the CC BY-NC-ND license (http://creativecommons.org/licenses/by-nc-nd/4.0/).

3.3. NNT reverse mode of operation increases the islet sensitivity to exogenous H_2O_2 at low glucose

To further evaluate how a lack of NNT affects cytosolic and mitochondrial redox state in β-cells, we compared the effect of low concentrations of exogenous H_2O_2 on (mt)-GRX1-roGFP2 oxidation in N- and J-islets. Figure 3 shows that the cytosolic and mitochondrial probes were less sensitive to H_2O_2 in the presence of G10 than G2, indicating that glucose improved the antioxidant defenses in both compartments. At G10, the traces were similar in both islet types (Figure 3A and C), suggesting that NNT did not protect β-cells against H_2O_2. In contrast, at G2, mt-GRX1-roGFP2 oxidation was lower in J- than N-islets in the presence of up to 10 μmol/l H_2O_2. More surprisingly, oxidation of cytosolic GRX1-roGFP2 occurred at slightly lower H_2O_2 concentrations in N- *vs.* J-islets. These results suggested that, at low glucose, the lack of NNT protects the mitochondrial matrix and also, to a limited extent, the cytosol against low concentrations of H_2O_2. This conclusion is further supported by Figure 3E showing that the oxidation of GRX1-roGFP2 by 10 μmol/l H_2O_2, which was similar in both islet types in the presence of G10 or G30, increased to a significantly larger extent upon glucose deprivation in N- than J-islets.

3.4. The reduction of GSIS in J-islets lies at a step distal to Ca^{2+} influx

In other experimental models, the negative impact of reduced NNT activity on GSIS was attributed to mitochondrial oxidative stress, with reduced ATP production and lack of Ca^{2+} rise upon glucose stimulation [13,14]. As these results were discordant with our data showing similar glucose-induced rise in NADH/NAD(H) ratio in J- and N-islets (Figure 1C), we reinvestigated glucose tolerance, islet GSIS and stimulus-secretion coupling in J- and N-mice, focusing on mitochondrial events involved in the triggering pathway of GSIS. Figure 4A shows that blood glucose levels were higher in J- than N-mice in the fed state, after overnight fasting and after 1 h refeeding, in agreement with most [13,14,28] but not all [29] previous studies. In static incubations of isolated islets, GSIS was reduced by 60—70% in J-islets, while it was not different in N/J- *vs.* N-islets (Figure 4B). In perifusion experiments (Figure 4C), the first and second phases of GSIS were also reduced by ~60—70% in J-islets, with a flat second phase in comparison with the slowly ascending phase in N-islets. However, GSIS was reduced despite almost identical glucose stimulation of the triggering pathway, as the glucose-induced changes in ^{14}C-glucose oxidation, mitochondrial matrix pH, mitochondrial membrane potential, OCR, ATP/(ATP + ADP) ratio and $[Ca^{2+}]_i$ were similar in both islet types (Figure 4D—I). These results suggested that the secretory defect of J-islets resulted from alterations in Ca^{2+}-induced exocytosis or its metabolic amplification downstream the triggering pathway of GSIS.

3.5. Metabolic amplification of GSIS in J- *vs.* N-islets

Under control conditions, GSIS was reduced in J- *vs.* N-islets between G15 and G30 despite their similar insulin content (Figure 5A). When islets were depolarized by 30 mmol/l extracellular K^+ (K30) in the presence of the K_{ATP}-channel opener diazoxide (Dz) to test the metabolic amplifying pathway of GSIS [1], $[Ca^{2+}]_i$ was similarly increased in both islet types (Figure S5), but the rate of insulin secretion was significantly lower in J- than N-islets (~60—70% reduction between G0.5 and G20, ~50% reduction at G30) (Figure 5B). Under these conditions, glucose still amplified depolarization-induced insulin secretion in J-islets, but to a lower

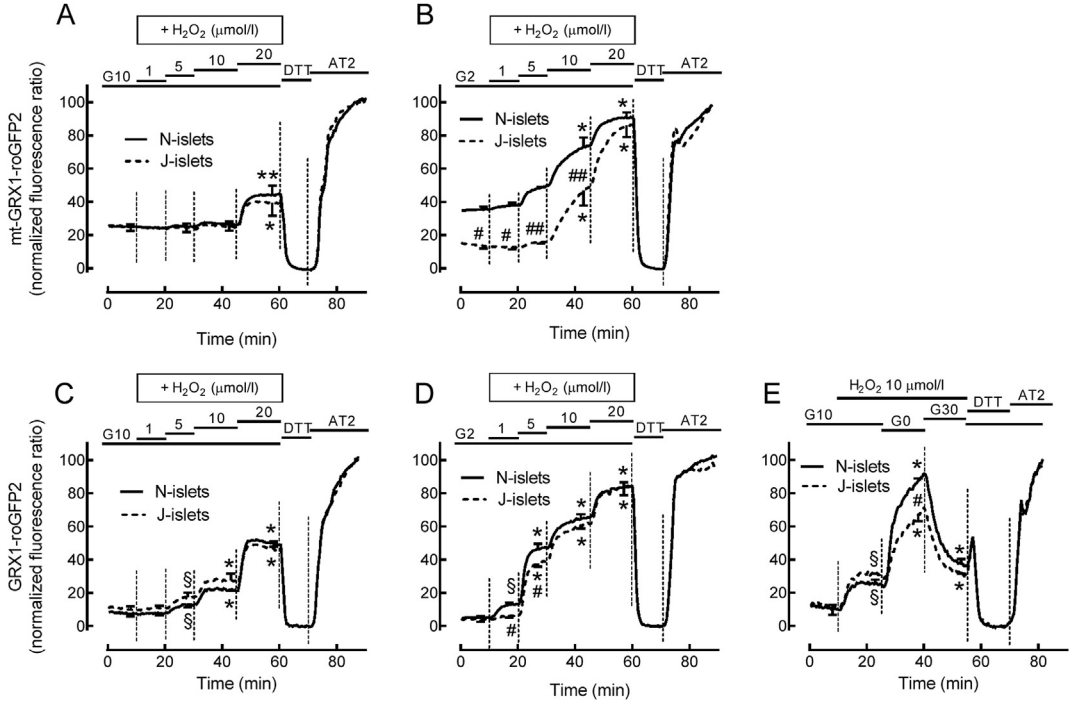

Figure 3: Effects of H_2O_2 on mitochondrial and cytosolic glutathione oxidation in N- and J-islets. Islets were perifused in the presence of increasing concentrations of exogenous H_2O_2 at different glucose concentrations (Gn = n mmol/l glucose), as shown at the top of the graphs. The traces were normalized as in Figure 2. Data are means ± SEM for n islet preparations. A and B, islets infected with Ad-mt-GRX1-roGFP2. C-E, islets infected with Ad-GRX1-roGFP2. A, $*P < 0.01$, $**P < 0.0001$ *vs.* G10 alone (n = 3). B, $*P < 0.0001$ *vs.* G2 alone; $\#P < 0.05$, $\#\#P < 0.001$ *vs.* N-islets (n = 4). C, $\S P < 0.05$, $*P < 0.0001$ *vs.* G10 alone (n = 4). D, $\S P < 0.05$, $*P < 0.0001$ *vs.* G2 alone; $\#P < 0.05$ *vs.* N-islets when analyses were restricted to data at 0, 1 and 5 μmol/l H_2O_2 (n = 3). E, $\S P < 0.05$, $*P < 0.0001$ *vs.* previous step; $\#P < 0.001$ *vs.* N-islets (n = 3).

 © 2017 The Authors. Published by Elsevier GmbH. This is an open access article under the CC BY-NC-ND license (http://creativecommons.org/licenses/by-nc-nd/4.0/).

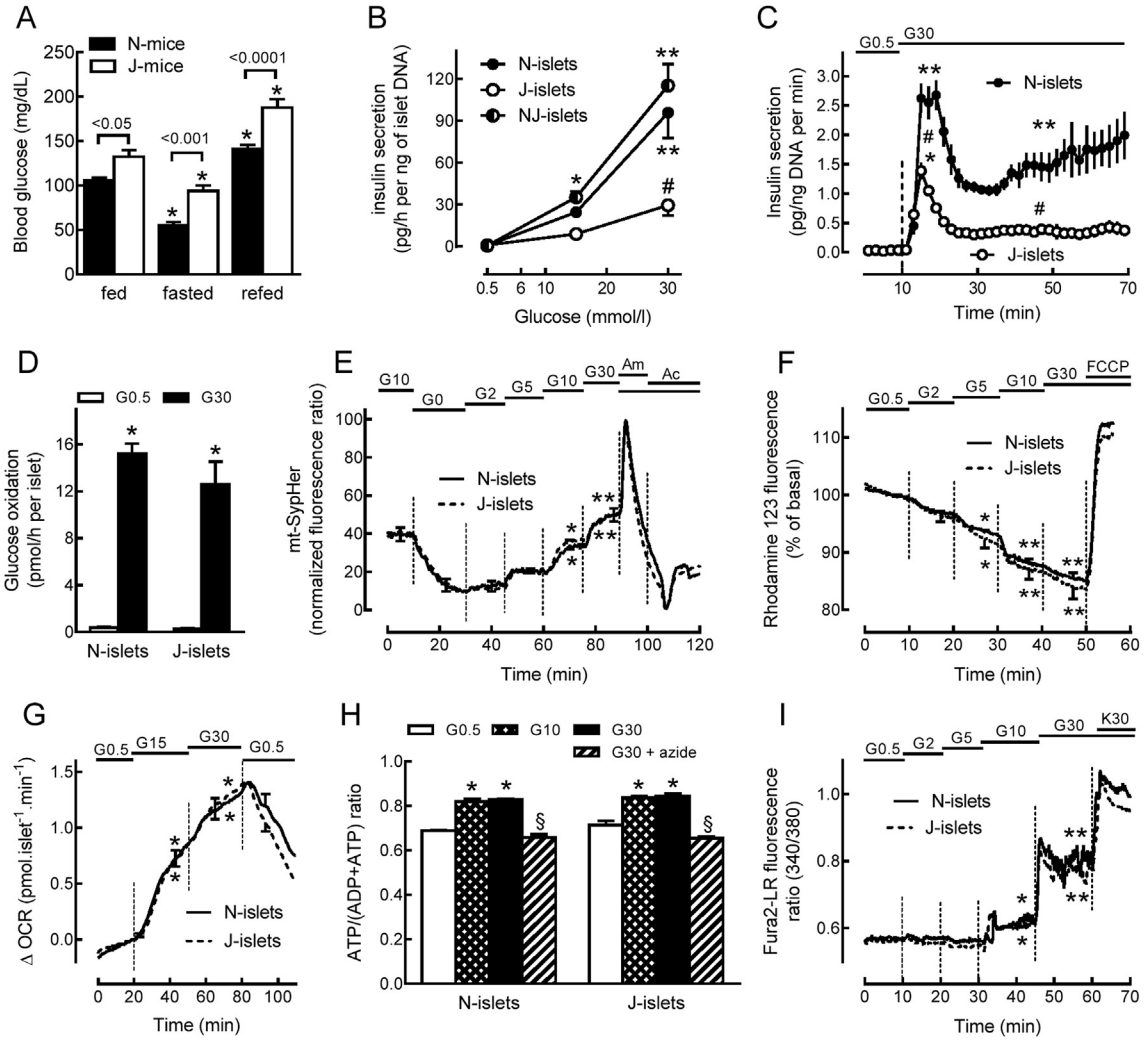

Figure 4: Glucose tolerance, GSIS and stimulus-secretion coupling events in N- and J-islets. A, blood glucose in female N- and J-mice under fed conditions (sampling at 9 AM) and after an overnight fast without or with 1 h refeeding (n = 5). *$P < 0.0001$ *vs.* fed state. Shown are *P* values for the differences between N and J mice. B–I, islets were incubated or perifused at various glucose concentrations and in the presence of 30 mmol/l ammonium chloride (Am), 30 mmol/l Na^{+}-acetate (Ac), 5 mmol/l azide or 10 μmol/l FCCP. Data are means ± SEM for n islet preparations. B, GSIS in N-, N/J- and J-islets. The insulin to DNA content ratio was 0.65 ± 0.08 ng/ng in N-islets, 0.75 ± 0.11 ng/ng in J-islets, and 0.65 ± 0.09 ng/ng in N/J-islets. *$P < 0.05$, **$P < 0.0001$ *vs.* G0.5; #$P < 0.0001$ *vs.* N-islets (n = 4). C, dynamic GSIS in N- and J-islets. The insulin to DNA content ratio was 1.62 ± 0.22 ng/ng in N-islets and 1.56 ± 0.18 ng/ng in J-islets. Statistical analysis was done on the area under the curve for first phase (min 10-25) and second phase (min 25–70) of GSIS. *$P < 0.01$, **$P < 0.0001$ *vs.* G0.5; #$P < 0.0001$ *vs.* N-islets (n = 4). D, ^{14}C-glucose oxidation in N- and J-islets during 2 h incubation. *$P < 0.0001$ *vs.* G0.5 (n = 3). E, mt-SypHer fluorescence ratio, an indicator of mitochondrial pH, normalized to its maximum value in Am and minimum value in Ac. *$P < 0.001$, **$P < 0.0001$ *vs.* G0 (n = 3). F, rhodamine 123 fluorescence normalized to its initial level in G0.5. *$P < 0.01$, **$P < 0.0001$ *vs.* G0.5 (n = 4). G, relative changes in OCR in perifused islets. *$P < 0.0001$ *vs.* G0.5 (n = 4). H, ATP/(ATP + ADP) ratio after 30 min incubation. *$P < 0.0001$ *vs.* G0.5; §$P < 0.001$ *vs.* G30 (n = 3). I, Fura2-LR fluorescence ratio in N- and J-islets loaded for 2 h with the Ca^{2+} probe (2 μmol/l). *$P < 0.05$, **$P < 0.0001$ *vs.* G0.5 (n = 4).

 © 2017 The Authors. Published by Elsevier GmbH. This is an open access article under the CC BY-NC-ND license (http://creativecommons.org/licenses/by-nc-nd/4.0/).

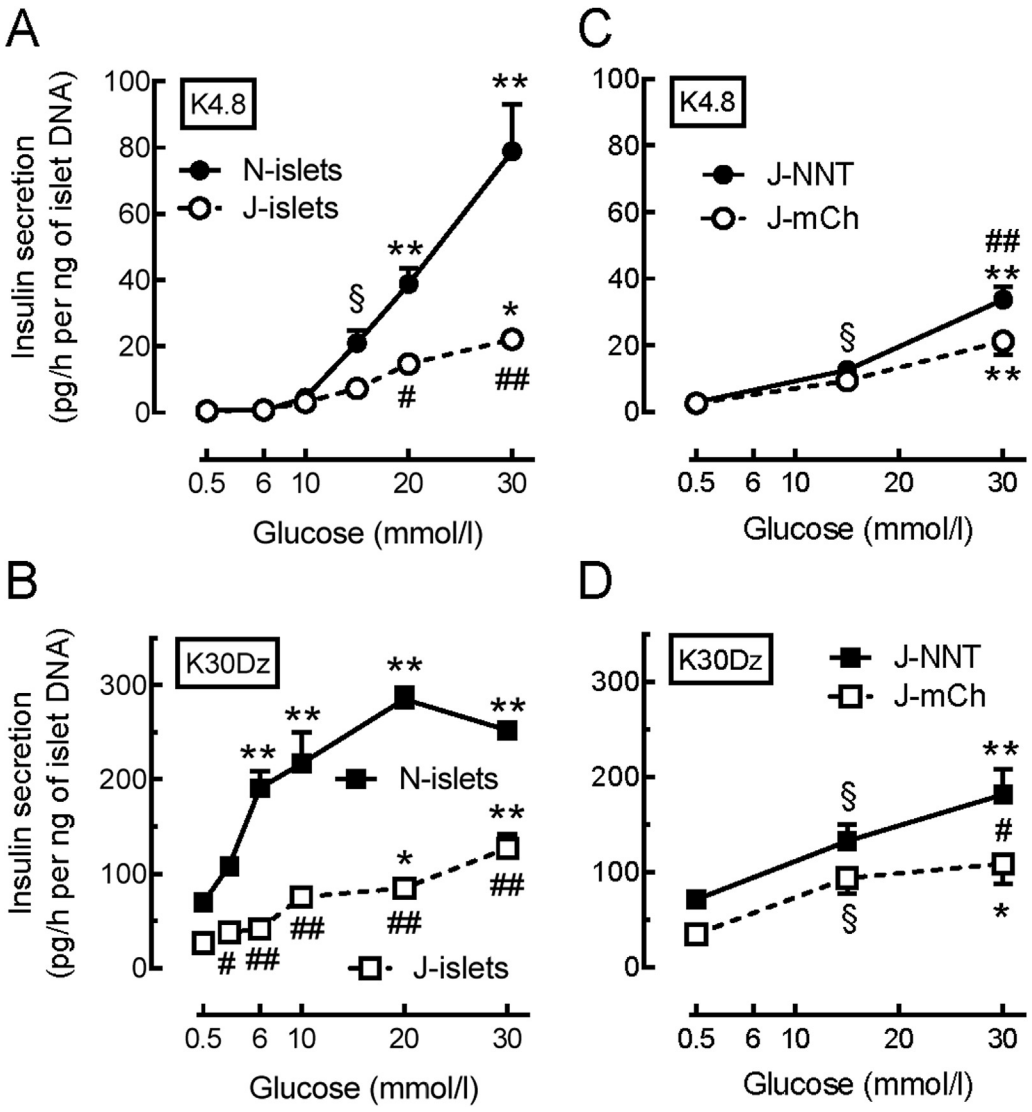

Figure 5: Metabolic amplification of insulin secretion in N-islets, J-islets, and J-islets infected with Ad-NNT. N- and J-islets were incubated for 1 h at increasing glucose concentrations under control (A, C, E) or depolarizing (B, D, F) conditions (Kn, n mmol/l extracellular K^+; Dz, 250 μmol/l diazoxide). The incubations were done in parallel under both conditions on the same islet preparations. For each sample, the rate of insulin secretion was expressed relative to the islet DNA content. A and B, islet DNA content (A, 0.83 ± 0.02 in N-islets and 0.86 ± 0.05 in J-islets; B, 0.92 ± 0.03 in N-islets and 0.88 ± 0.05 in J-islets). Data are means ± SEM for 8–9 batches of 5 islets from 3 islet preparations. §$P < 0.05$, *$P < 0.01$, **$P < 0.0001$ *vs.* G0.5, #$P < 0.01$, ##$P < 0.0001$ *vs.* J-islets. C and D, 4 days before the experiment, J-islets were infected with Ad-NNT (J-NNT) or Ad-mCh (J-mCh) as control. Islet DNA content (C, 0.70 ± 0.05 in J-NNT-islets and 0.49 ± 0.02 in J-mCh islets; D, 0.69 ± 0.03 in J-NNT-islets and 0.65 ± 0.06 in J-mCh-islets). Data are means ± SEM for 11–12 batches of 5 islets from 4 islet preparations. §$P < 0.05$, *$P < 0.01$, **$P < 0.0001$ *vs.* G0.5, #$P < 0.05$, ##$P < 0.01$ *vs.* J-mCh islets.

extent than in N-islets. These results indicated that the lack of NNT markedly reduced Ca^{2+}-induced exocytosis and its metabolic amplification.

3.6. Impact of WT NNT expression on GSIS in J-islets

It was previously shown that expression of WT NNT in J-mice corrects their defect in GSIS [14]. Here, GSIS was not reduced in NJ-islets (Figure 4B), showing that one WT allele of *Nnt* suffices to preserve β-cell secretory function. We nevertheless tested the impact of WT NNT expression on GSIS in J-islets. Figure 5C–D shows that infection of J-islets with Ad-NNT reduced the difference in GSIS between J- and N-islets to a similar extent as it restored the decrease in NADPH/NADP(H) ratio in G0.5 *vs.* G30 in Figure 1F, by ~20–25% under control conditions and ~40–60% under depolarizing conditions. However, infecting J-islet with Ad-NNT after gentle trypsinization did not increase GSIS (Figure S6A and B).

3.7. Metabolite profiling of resting and glucose-stimulated N- and J-islets

Given the strong reduction of GSIS despite the apparent preservation of glucose metabolism in J- *vs.* N-islets, we examined the relative changes in metabolite levels in response to glucose stimulation, using untargeted GC/MS analysis. Figure 6 shows that N- and J-islets displayed similar changes in most glycolytic and Krebs cycle intermediates, e.g.

 © 2017 The Authors. Published by Elsevier GmbH. This is an open access article under the CC BY-NC-ND license (http://creativecommons.org/licenses/by-nc-nd/4.0/).

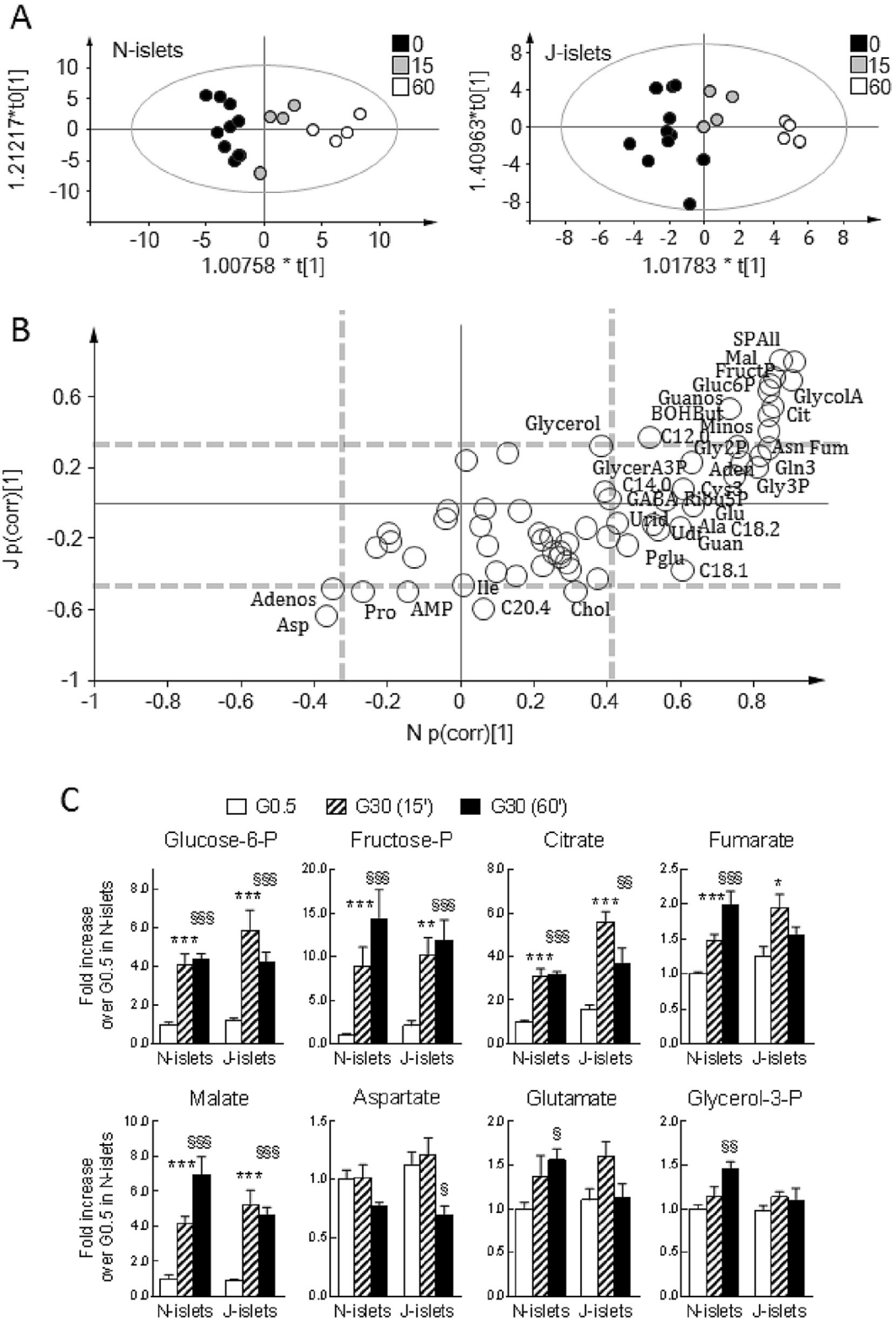

Figure 6: Metabolite profiling of N- and J-islets. A, score scatter plots from OPLS-DA models calculated with the time (0—15—60 min) of glucose stimulation (G30) as discriminating variable. Samples cluster according to time in stimulatory glucose for both N- (left) and J- (right) islets. B, loadings from the OPLS-DA models combined in a shared and unique structure-like plot (SUS-like plot). Metabolites from glycolysis and the Krebs cycle increase with time in stimulatory glucose levels in both N- and J-islets (upper right corner). However, intermediates involved in mitochondrial shuttling, glutamate and glycerol-3-phosphate, increase only in N-islets. C, normalized metabolite levels at basal and 15 and 60 min after glucose stimulation in N- and J-islets confirms glucose unresponsiveness in mitochondrial shuttle intermediates. Data are means ± SEM for 10 samples in G0.5 and 4 samples in G30 for both N- and J-islets. Differences between groups were assessed by one-way ANOVA, followed by Tukey's multiple comparison test post hoc. $*P < 0.05$, $**P < 0.01$, $***P < 0.001$, for 15 min G30 *vs.* G0.5, and $\S P < 0.05$, $\S\S P < 0.01$, $\S\S\S P < 0.001$, for 60 min G30 *vs.* G0.5.

 © 2017 The Authors. Published by Elsevier GmbH. This is an open access article under the CC BY-NC-ND license (http://creativecommons.org/licenses/by-nc-nd/4.0/).

increased levels of glucose-6-phosphate, fructose phosphate, citrate and malate, and a decrease in aspartate levels. However, the rise in the level of intermediates involved in mitochondrial shuttling, i.e. glycerol-3-phosphate (Gly3P) at 15 and 60 min, as well as glutamate levels at 60 min of G30 stimulation, was clearly defective (Figure 6).

4. DISCUSSION

In this study, we show that NNT is largely responsible for the glucose-induced rise in NADPH/NADP(H) ratio and decrease in mitochondrial glutathione redox state in mouse pancreatic islets. However, in the physiological range of glucose concentrations, this effect resulted from a reduction in NADPH consumption by NNT reverse mode of operation, rather than from a stimulation of NADPH production by the enzyme (Figure 7). At non-stimulating glucose, such reverse mode of NNT operation increased the sensitivity of N-islets to exogenous H_2O_2 in the mitochondrial matrix and, to a small extent, the cytosol. Finally, we show that long-term lack of NNT did not alter the glucose-induced rise in $[Ca^{2+}]_i$ and upstream coupling events, but that it markedly reduced GSIS by altering the efficacy of Ca^{2+} on exocytosis and its metabolic amplification.

4.1. Islet NNT mode of operation

The glucose-induced rise in cytosolic NADPH/NADP(H) ratio was previously proposed as a metabolic coupling factor controlling GSIS in association with GRX1 [5,6]. Recently, we showed that the increase in NAD(P)H autofluorescence correlates with a decrease in mitochondrial glutathione oxidation in rat and human β-cells, while cytosolic glutathione oxidation was low at all glucose concentrations, suggesting that mitochondrial glutathione redox state could play a role in GSIS [11].

In this study, comparing islets with and without functional NNT unexpectedly revealed that most of the glucose-induced rise in islet NADPH/NADP(H) ratio did not result from a progressive increase in NADPH production but from a progressive reduction in NADPH consumption by NNT reverse mode of operation between G0 and G30. Accordingly, this was responsible for the glucose-mediated decrease in mitochondrial glutathione oxidation in β-cells.

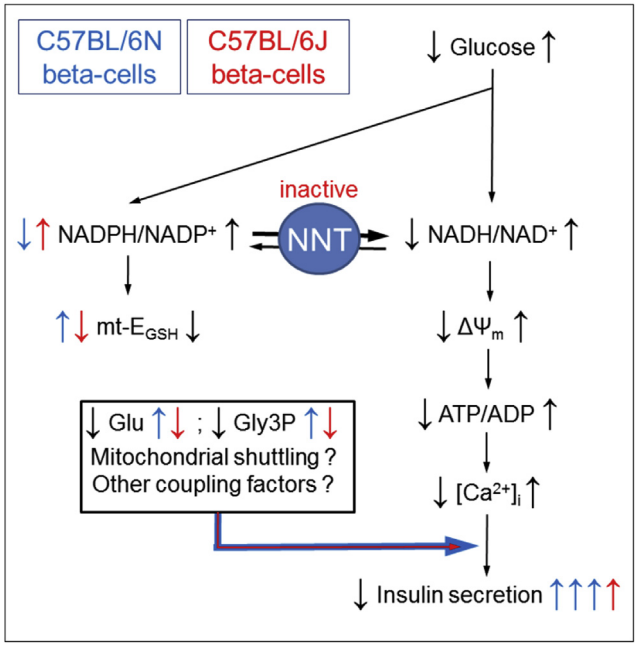

Figure 7: Impact of a lack of NNT on metabolic parameters (potentially) involved in GSIS in mouse pancreatic β-cells. Arrows on the left, level at non-stimulating [glucose]; arrows on the right, level at stimulating [glucose]; ↑, high levels; ↓, low levels. Blue and red arrows highlight differences between N and J-islets. Differences in the amplitude of GSIS is depicted by different arrow numbers.

Our conclusion that islet NNT operates in the reverse mode relies on the higher NADPH/NADP(H) ratio and lower mitochondrial glutathione oxidation in J- than N-islets at non-stimulating glucose. We excluded the possibility that this difference resulted from the adaptation of J-islets to long-term mitochondrial oxidative stress, since it was abrogated after 2–4 days of WT NNT expression, indicating that NNT rapidly operates in the reverse mode once expressed in β-cells. These results also rule out the possibility that these differences between J- and N-islets result from other genetic differences [25,30,31].

It may seem surprising that NNT can operate in the reverse mode at physiological glucose concentrations. However, β-cells are unique in their ability to modulate their metabolic rate according to the glucose concentration. This is usually presented as an ability to increase their NADH/NAD^+ ratio, mitochondrial proton motive force (depending on both mitochondrial membrane potential and pH gradient), and ATP/ADP ratio upon glucose stimulation, but it might be more correct to state, as recently pointed out in a review on β-cell mitochondria [4], that β-cells allow these parameters to drop below 10 mmol/l glucose. Such unusual behavior could be related to the low coupling efficiency of β-cell mitochondria [4,32]. A low NADH/NAD^+ ratio, mitochondrial proton motive force, and ATP/ADP ratio, as observed in β-cells at non-stimulating glucose, correspond to the conditions that activate NNT reverse mode of operation in mitochondria isolated from other tissues [33,34]. In the presence of increasingly higher glucose concentrations, the islet mitochondrial NADH/NAD^+ ratio, proton motive force and ATP/ADP ratio progressively increase, and NNT reverse mode of operation is expected to decrease until it eventually reverts to the forward mode. The glucose concentration around which NNT mode of operation switches from reverse to forward is expected to depend on the proton motive force and the NADH/NAD^+ and NADPH/$NADP^+$ ratios [35]. We first estimated it at or above 10 mM glucose, a condition under which β-cell NADH/NAD^+ ratio, mitochondrial proton motive force and ATP/ADP ratio are high and similar to those observed in most cell types under energized conditions [4]. However, it may be closer to 30 mM glucose, as even at this very high glucose concentration, the islet NADPH/NADP(H) ratio was not lower and mitochondrial glutathione was not more oxidized in J-islets, suggesting that NNT did not contribute to the maintenance of the high NADPH/NADP(H) ratio. Moreover, our estimation of NADPH consumption by NNT suggests that it is only fully suppressed at about G30. Nevertheless, given the uncertainties of the above estimation and the slightly higher absolute NADPH autofluorescence level in N-islets at G30 (see Figure 1A and B), we cannot exclude the possibility that islet NNT operates in the forward mode above G10, as it does in most cell types under control conditions [15,33,34]. Figure S7 schematizes the impact of NNT mode of operation on islet NADP and glutathione redox state at varying glucose concentrations.

4.2. Consequences of NNT reverse mode of operation on β-cell oxidative stress

The lack of functional NNT had a strong impact on islet NADPH/NADP(H) ratio and mitochondrial glutathione oxidation at low but not intermediate and high glucose. J-islets may therefore be protected against low glucose-induced mitochondrial oxidative stress [18,36,37]. In contrast, there was no significant impact of the lack of NNT on cytosolic glutathione oxidation at physiological glucose concentrations. However, at very low glucose or in its complete absence, cytosolic glutathione oxidation tended to be lower in J-islets both in the absence

 © 2017 The Authors. Published by Elsevier GmbH. This is an open access article under the CC BY-NC-ND license (http://creativecommons.org/licenses/by-nc-nd/4.0/).

or presence of exogenous H_2O_2, suggesting that a lack of NNT reverse mode of operation could also protect β-cells from cytosolic oxidative stress when glucose metabolism is strongly reduced. Such a paradoxical effect in which the lack of NNT protects from cellular oxidative stress has been recently reported in cardiomyocytes from mice submitted to chronic trans-aortic constriction and in brain cells exposed to ischemia-reperfusion damage [34,38]. However, NNT only slightly modulated the large increase in H_2O_2 sensitivity triggered in the cytosol of both islet types by a reduction in glucose from G10 to G2. On the other hand, if NNT operates in the normal mode at high glucose, J-islets should be more sensitive to high glucose-induced mitochondrial oxidative stress, in agreement with the observation that many other cell types are more prone to oxidative stress in J- than N-mice [33,39–41].

4.3. NNT and GSIS

In contrast with previous studies [13,42], long-term lack of NNT did not alter other aspects of mitochondrial metabolism associated with the triggering pathway of GSIS. Nevertheless, the lack of NNT markedly reduced both first and second phases of GSIS by altering the efficacy of Ca^{2+} on exocytosis and its metabolic amplification.

Our results in non-trypsinized J-islets showing that WT NNT expression restored GSIS to the same extent as it improved the glucose regulation of NADPH/NADP(H) ratio support the conclusion that the lack of NNT is responsible for the lower GSIS in J-islets. This is in agreement with a study demonstrating the ability of NNT expression in J-mice to restore their GSIS [14]. The surprising observation that NNT expression in trypsinized J-islets did not increase GSIS despite its ability to fully restore the glucose-induced changes in NADPH/NADP(H) ratio and mitochondrial glutathione oxidation may result from a negative impact of trypsinization on the regulation of GSIS. We cannot, however, totally exclude the possibility that the lower GSIS in J-islets also results, in part, from long-term β-cell adaptation to the lack of NNT in the whole organism. J-mice have indeed a 50% lower plasma corticosterone level than N-mice [43] and display an increase in oxidative stress with compensatory increase in antioxidant defenses in various cell types involved in glucose homeostasis [41]. Formal testing of that hypothesis will require a model of conditional NNT deletion in adult β-cells. In humans, NNT mutations are a cause of familial glucocorticoid deficiency [43], and a recent study reported that one patient suffering from this condition developed non-autoimmune diabetes at the age of 10, suggesting that, depending on the genetic environment and the presence of other gene variants, NNT mutation may lead to a defect in insulin secretion [44].

How does the lack of NNT reduce GSIS in J-islets? A previously considered explanation, that it induces mitochondrial oxidative stress with loss of the glucose-induced rise in ATP production and $[Ca^{2+}]_i$ [13,15,42], was not confirmed in this study. Thus, lower GSIS in J- *vs.* N-islets resulted from a defect in Ca^{2+}-induced exocytosis and its metabolic amplification. Such discordant results between studies may have resulted from the use of different experimental models; we compared stimulus-secretion coupling events in N- and J-islets from mice with similar genetic background, while previous studies compared islets from J-mice and genetically unrelated C3H/HeH, DBA/2 and BALB/c mice. A second hypothesis, that GSIS is lower because NADPH is lower or oxidation of cytosolic and mitochondrial glutathione is higher at stimulating glucose concentrations, was also invalidated by our data, at least up to G10. We then considered the possibility that metabolic fluxes are reduced in J-islets despite their similar steady-state levels of ATP and NADH, but the similar glucose stimulation of OCR, glucose oxidation and accumulation of glycolytic and Krebs cycle intermediates, argued against it. Finally, we found that J-islets have a defect in the glucose-induced accumulation of metabolites involved in mitochondrial shuttles, i.e. in Gly3P and Glu, which may play a role in GSIS [2]. The lack of increase in Gly3P could alter the glycerol-phosphate shuttle, which transfers reducing equivalent from the cytosol to the mitochondria and is particularly active in pancreatic islets [45], or the production of mono-, di- and tri-acylglycerol impacting PKC activation or other still poorly understood aspects of GSIS [46]. Thus, the link between a lack of NNT, these metabolic alterations, and the reduction of GSIS remains unclear (Figure 7).

4.4. C57BL/6J mice

Whether C57BL/6J mice are useful to study oxidative stress and glucose homeostasis has been raised since the discovery of their NNT mutation and its impact on glucose tolerance and the phenotype of SOD2-KO mice [13,14,47]. Recent papers [25,34,41,48,49] reemphasized that J-mice may not be a valid model to study the pathophysiology of human diseases, except for studies on NNT mutations associated with familial glucocorticoid deficiency with possible development of diabetes later in life [43,44,50]. Our study further supports the idea that J-mice should be avoided as control mice. Meanwhile, the NNT genotype of C57BL/6 mice should be systematically reported.

5. CONCLUSION

NNT operates in the reverse mode in insulin-secreting β-cells, thereby lowering islet NADPH levels and increasing mitochondrial glutathione oxidation at non-stimulating *vs.* stimulating glucose concentrations. The lack of NNT in islets from C57BL/6J mice does not detectably alter other aspects of mitochondrial metabolism associated with the triggering pathway of GSIS but markedly reduces both first and second phases of GSIS by altering Ca^{2+}-induced exocytosis and its metabolic amplification.

AUTHOR'S CONTRIBUTIONS

LRBS, CM, HKT, and JCJ conceived the study and designed the experiments. LRBS, CM, AHS, HKT, and HC performed the experiments and analysed the data, except for OCR measurements (IRS) and GC/MS analysis (PS and HM). LRBS, CM, and JCJ wrote the paper, other authors edited and approved it.

ACKNOWLEDGEMENTS

We thank Dr. Ting–Ting Huang (Stanford Neuroscience Institute, CA) for mouse NNT antibody, and Dr. Decio L. Eizirik (Université Libre de Bruxelles, Belgium) for the protocol of adenoviral infection after gentle trypsinization.

JCJ is Research Director of the Fonds de la Recherche Scientifique-FNRS, Belgium. AHS was a recipient of scholarship abroad (BEPE-DR #2013/18232-5) from São Paulo Research Foundation (FAPESP).

This study was funded by Action de Recherche Concertée 12/17-047 from the Communauté française de Belgique, Grant 3.4521.12 from the Fonds de la Recherche Scientifique Médicale, and Grant SFD/MSD 2016 from the Société Francophone du Diabète (Paris, France) to JCJ, and the National Institutes of Health Grant DK17047 (the DRC Cell Function Analysis Core) to IRS. An equipment grant from Knut and Alice Wallenberg's Foundation is acknowledged.

CONFLICT OF INTEREST

The authors declare that they have no conflict of interest.

 © 2017 The Authors. Published by Elsevier GmbH. This is an open access article under the CC BY-NC-ND license (http://creativecommons.org/licenses/by-nc-nd/4.0/).

APPENDIX A. SUPPLEMENTARY DATA

Supplementary data related to this article can be found at http://dx.doi.org/10.1016/j.molmet.2017.04.004.

REFERENCES

[1] Henquin, J.C., 2000. Triggering and amplifying pathways of regulation of insulin secretion by glucose. Diabetes 49:1751–1760.

[2] Maechler, P., 2013. Mitochondrial function and insulin secretion. Molecular and Cellular Endocrinology 379:12–18.

[3] Prentki, M., Matschinsky, F.M., Madiraju, S.R., 2013. Metabolic signaling in fuel-induced insulin secretion. Cell Metabolism 18:162–185.

[4] Nicholls, D.G., 2016. The pancreatic beta-cell: a bioenergetic perspective. Physiological Reviews 96:1385–1447.

[5] Ivarsson, R., Quintens, R., Dejonghe, S., Tsukamoto, K., In't Veld, P.A., Renstrom, E., et al., 2005. Redox control of exocytosis: regulatory role of NADPH, thioredoxin, and glutaredoxin. Diabetes 54:2132–2142.

[6] Reinbothe, T.M., Ivarsson, R., Li, D.Q., Niazi, O., Jing, X., Zhang, E., et al., 2009. Glutaredoxin-1 mediates NADPH-dependent stimulation of calcium-dependent insulin secretion. Molecular Endocrinology 23:893–900.

[7] Spegel, P., Sharoyko, V.V., Goehring, I., Danielsson, A.P., Malmgren, S., Nagorny, C.L., et al., 2013. Time-resolved metabolomics analysis of beta-cells implicates the pentose phosphate pathway in the control of insulin release. Biochemical Journal 450:595–605.

[8] Gooding, J.R., Jensen, M.V., Dai, X., Wenner, B.R., Lu, D., Arumugam, R., et al., 2015. Adenylosuccinate is an insulin secretagogue derived from glucose-induced purine metabolism. Cell Reports 13:157–167.

[9] Ferdaoussi, M., Dai, X., Jensen, M.V., Wang, R., Peterson, B.S., Huang, C., et al., 2015. Isocitrate-to-SENP1 signaling amplifies insulin secretion and rescues dysfunctional beta cells. The Journal of Clinical Investigation 125:3847–3860.

[10] Patterson, G.H., Knobel, S.M., Arkhammar, P., Thastrup, O., Piston, D.W., 2000. Separation of the glucose-stimulated cytoplasmic and mitochondrial NAD(P)H responses in pancreatic islet beta cells. Proceedings of the National Academy of Sciences of the United States of America 97:5203–5207.

[11] Takahashi, H.K., Santos, L.R., Roma, L.P., Duprez, J., Broca, C., Wojtusciszyn, A., et al., 2014. Acute nutrient regulation of the mitochondrial glutathione redox state in pancreatic beta-cells. Biochemical Journal 460:411–423.

[12] Jitrapakdee, S., Wutthisathapornchai, A., Wallace, J.C., MacDonald, M.J., 2010. Regulation of insulin secretion: role of mitochondrial signalling. Diabetologia 53:1019–1032.

[13] Toye, A.A., Lippiat, J.D., Proks, P., Shimomura, K., Bentley, L., Hugill, A., et al., 2005. A genetic and physiological study of impaired glucose homeostasis control in C57BL/6J mice. Diabetologia 48:675–686.

[14] Freeman, H.C., Hugill, A., Dear, N.T., Ashcroft, F.M., Cox, R.D., 2006. Deletion of nicotinamide nucleotide transhydrogenase: a new quantitive trait locus accounting for glucose intolerance in C57BL/6J mice. Diabetes 55:2153–2156.

[15] Rydstrom, J., 2006. Mitochondrial NADPH, transhydrogenase and disease. Biochimica et Biophysica Acta 1757:721–726.

[16] Leung, J.H., Schurig-Briccio, L.A., Yamaguchi, M., Moeller, A., Speir, J.A., Gennis, R.B., et al., 2015. Structural biology. Division of labor in transhydrogenase by alternating proton translocation and hydride transfer. Science 347:178–181.

[17] Kim, A., Chen, C.H., Ursell, P., Huang, T.T., 2010. Genetic modifier of mitochondrial superoxide dismutase-deficient mice delays heart failure and prolongs survival. Mammalian Genome 21:534–542.

[18] Roma, L.P., Pascal, S.M., Duprez, J., Jonas, J.C., 2012. Mitochondrial oxidative stress contributes differently to rat pancreatic islet cell apoptosis and insulin secretory defects after prolonged culture in a low non-stimulating glucose concentration. Diabetologia 55:2226–2237.

[19] Quoix, N., Cheng-Xue, R., Guiot, Y., Herrera, P.L., Henquin, J.C., Gilon, P., 2007. The GluCre-ROSA26EYFP mouse: a new model for easy identification of living pancreatic α-cells. FEBS Letters 581:4235–4240.

[20] Roma, L.P., Duprez, J., Jonas, J.C., 2015. Glucokinase activation is beneficial or toxic to cultured rat pancreatic islets depending on the prevailing glucose concentration. American Journal of Physiology. Endocrinology and Metabolism 309:E632–E639.

[21] Khaldi, M.Z., Guiot, Y., Gilon, P., Henquin, J.C., Jonas, J.C., 2004. Increased glucose sensitivity of both triggering and amplifying pathways of insulin secretion in rat islets cultured for one week in high glucose. American Journal of Physiology. Endocrinology and Metabolism 287:E207–E217.

[22] Gutscher, M., Pauleau, A.L., Marty, L., Brach, T., Wabnitz, G.H., Samstag, Y., et al., 2008. Real-time imaging of the intracellular glutathione redox potential. Nature Methods 5:553–559.

[23] Sweet, I.R., Cook, D.L., DeJulio, E., Wallen, A.R., Khalil, G., Callis, J., et al., 2004. Regulation of ATP/ADP in pancreatic islets. Diabetes 53:401–409.

[24] Jung, S.R., Kuok, I.T., Couron, D., Rizzo, N., Margineantu, D.H., Hockenbery, D.M., et al., 2011. Reduced cytochrome C is an essential regulator of sustained insulin secretion by pancreatic islets. The Journal of Biological Chemistry 286:17422–17434.

[25] Fontaine, D.A., Davis, D.B., 2016. Attention to background strain is essential for metabolic Research: C57BL/6 and the international knockout mouse consortium. Diabetes 65:25–33.

[26] Meyer, A.J., Dick, T.P., 2010. Fluorescent protein-based redox probes. Antioxidants & Redox Signaling 13:621–650.

[27] Cameron, W.D., Bui, C.V., Hutchinson, A., Loppnau, P., Graslund, S., Rocheleau, J.V., 2016. Apollo-NADP(+): a spectrally tunable family of genetically encoded sensors for NADP(+). Nature Methods 13:352–358.

[28] Fergusson, G., Ethier, M., Guevremont, M., Chretien, C., Attane, C., Joly, E., et al., 2014. Defective insulin secretory response to intravenous glucose in C57Bl/6J compared to C57Bl/6N mice. Molecular Metabolism 3:848–854.

[29] Wong, N., Blair, A.R., Morahan, G., Andrikopoulos, S., 2010. The deletion variant of nicotinamide nucleotide transhydrogenase (Nnt) does not affect insulin secretion or glucose tolerance. Endocrinology 151:96–102.

[30] Mekada, K., Abe, K., Murakami, A., Nakamura, S., Nakata, H., Moriwaki, K., et al., 2009. Genetic differences among C57BL/6 substrains. Experimental Animals 58:141–149.

[31] Simon, M.M., Greenaway, S., White, J.K., Fuchs, H., Gailus-Durner, V., Wells, S., et al., 2013. A comparative phenotypic and genomic analysis of C57BL/6J and C57BL/6N mouse strains. Genome Biology 14:R82.

[32] Wikstrom, J.D., Sereda, S.B., Stiles, L., Elorza, A., Allister, E.M., Neilson, A., et al., 2012. A novel high-throughput assay for islet respiration reveals uncoupling of rodent and human islets. PLoS One 7:e33023.

[33] Ronchi, J.A., Figueira, T.R., Ravagnani, F.G., Oliveira, H.C., Vercesi, A.E., Castilho, R.F., 2013. A spontaneous mutation in the nicotinamide nucleotide transhydrogenase gene of C57BL/6J mice results in mitochondrial redox abnormalities. Free Radical Biology and Medicine 63:446–456.

[34] Nickel, A.G., von, H.A., Hohl, M., Loffler, J.R., Kohlhaas, M., Becker, J., et al., 2015. Reversal of mitochondrial transhydrogenase causes oxidative stress in heart failure. Cell Metabolism 22:472–484.

[35] Hoek, J.B., Rydstrom, J., 1988. Physiological roles of nicotinamide nucleotide transhydrogenase. Biochemical Journal 254:1–10.

[36] Martens, G.A., Cai, Y., Hinke, S., Stange, G., Van de Casteele, M., Pipeleers, D., 2005. Glucose suppresses superoxide generation in metabolically responsive pancreatic β cells. The Journal of Biological Chemistry 280:20389–20396.

[37] Jonas, J.C., Bensellam, M., Duprez, J., Elouil, H., Guiot, Y., Pascal, S.M., 2009. Glucose regulation of islet stress responses and β-cell failure in type 2 diabetes. Diabetes, Obesity and Metabolism 11(Suppl. 4):65–81.

[38] Wolf, S., Hainz, N., Beckmann, A., Maack, C., Menger, M.D., Tschernig, T., et al., 2016. Brain damage resulting from postnatal hypoxic-ischemic brain

 © 2017 The Authors. Published by Elsevier GmbH. This is an open access article under the CC BY-NC-ND license (http://creativecommons.org/licenses/by-nc-nd/4.0/).

injury is reduced in C57BL/6J mice as compared to C57BL/6N mice. Brain Research 1650:224—231.

[39] Yin, F., Sancheti, H., Cadenas, E., 2012. Silencing of nicotinamide nucleotide transhydrogenase impairs cellular redox homeostasis and energy metabolism in PC12 cells. Biochimica et Biophysica Acta 1817:401—409.

[40] Lopert, P., Patel, M., 2014. Nicotinamide nucleotide transhydrogenase (Nnt) links the substrate requirement in brain mitochondria for hydrogen peroxide removal to the thioredoxin/peroxiredoxin (Trx/Prx) system. The Journal of Biological Chemistry 289:15611—15620.

[41] Fisher-Wellman, K.H., Ryan, T.E., Smith, C.D., Gilliam, L.A., Lin, C.T., Reese, L.R., et al., 2016. A direct comparison of metabolic responses to high-fat diet in C57BL/6J and C57BL/6NJ mice. Diabetes 65:3249—3261.

[42] Freeman, H., Shimomura, K., Cox, R.D., Ashcroft, F.M., 2006. Nicotinamide nucleotide transhydrogenase: a link between insulin secretion, glucose metabolism and oxidative stress. Biochemical Society Transactions 34:806—810.

[43] Meimaridou, E., Kowalczyk, J., Guasti, L., Hughes, C.R., Wagner, F., Frommolt, P., et al., 2012. Mutations in NNT encoding nicotinamide nucleotide transhydrogenase cause familial glucocorticoid deficiency. Nature Genetics 44: 740—742.

[44] Scott, R., Van, V.G., Deladoey, J., 2017. Association of adrenal insufficiency with insulin-dependent diabetes mellitus in a patient with inactivating mutations in nicotinamide nucleotide transhydrogenase: a phenocopy of the animal model. European Journal of Endocrinology 176:C1—C2.

[45] Eto, K., Tsubamoto, Y., Terauchi, Y., Sugiyama, T., Kishimoto, T., Takahashi, N., et al., 1999. Role of NADH shuttle system in glucose-induced activation of mitochondrial metabolism and insulin secretion. Science 283: 981—985.

[46] Attane, C., Peyot, M.L., Lussier, R., Poursharifi, P., Zhao, S., Zhang, D., et al., 2016. A beta cell ATGL-lipolysis/adipose tissue axis controls energy homeostasis and body weight via insulin secretion in mice. Diabetologia 59:2654—2663.

[47] Huang, T.T., Naeemuddin, M., Elchuri, S., Yamaguchi, M., Kozy, H.M., Carlson, E.J., et al., 2006. Genetic modifiers of the phenotype of mice deficient in mitochondrial superoxide dismutase. Human Molecular Genetics 15:1187—1194.

[48] Ronchi, J.A., Francisco, A., Passos, L.A., Figueira, T.R., Castilho, R.F., 2016. The contribution of nicotinamide nucleotide transhydrogenase to peroxide detoxification is dependent on the respiratory state and counterbalanced by other sources of NADPH in liver mitochondria. The Journal of Biological Chemistry 291:20173—20187.

[49] Attane, C., Peyot, M.L., Lussier, R., Zhang, D., Joly, E., Madiraju, S.R., et al., 2016. Differential insulin secretion of high-fat diet-fed C57BL/6NN and C57BL/6NJ mice: implications of mixed genetic background in metabolic studies. PLoS One 11:e0159165.

[50] Roucher-Boulez, F., Mallet-Motak, D., Samara-Boustani, D., Jilani, H., Ladjouze, A., Souchon, P.F., et al., 2016. NNT mutations: a cause of primary adrenal insufficiency, oxidative stress and extra-adrenal defects. European Journal of Endocrinology 175:73—84.

 © 2017 The Authors. Published by Elsevier GmbH. This is an open access article under the CC BY-NC-ND license (http://creativecommons.org/licenses/by-nc-nd/4.0/).